



# Molecular and Functional Characterization of Choline Transporter-Like Proteins in Esophageal Cancer Cells and Potential Therapeutic Targets

Fumiaki Nagashima<sup>1</sup>, Ryohta Nishiyama<sup>1</sup>, Beniko Iwao<sup>2</sup>, Yuiko Kawai<sup>3</sup>, Chikanao Ishii<sup>3</sup>, Tsuyoshi Yamanaka<sup>4</sup>, Hiroyuki Uchino<sup>1</sup> and Masato Inazu<sup>3,4,\*</sup>

Departments of <sup>1</sup>Anesthesiology, <sup>2</sup>Psychiatry, Tokyo Medical University, Tokyo 160-0023,

<sup>3</sup>Institute of Medical Science, <sup>4</sup>Department of Molecular Preventive Medicine, Tokyo Medical University, Tokyo 160-8402, Japan

## Abstract

In this study, we examined the molecular and functional characterization of choline uptake in the human esophageal cancer cells. In addition, we examined the influence of various drugs on the transport of [<sup>3</sup>H]choline, and explored the possible correlation between the inhibition of choline uptake and apoptotic cell death. We found that both choline transporter-like protein 1 (CTL1) and CTL2 mRNAs and proteins were highly expressed in esophageal cancer cell lines (KYSE series). CTL1 and CTL2 were located in the plasma membrane and mitochondria, respectively. Choline uptake was saturable and mediated by a single transport system, which is both Na<sup>+</sup>-independent and pH-dependent. Choline uptake and cell viability were inhibited by various cationic drugs. Furthermore, a correlation analysis of the potencies of 47 drugs for the inhibition of choline uptake and cell viability showed a strong correlation. Choline uptake inhibitors and choline deficiency each inhibited cell viability and increased caspase-3/7 activity. We conclude that extracellular choline is mainly transported via a CTL1. The functional inhibition of CTL1 by cationic drugs could promote apoptotic cell death. Furthermore, CTL2 may be involved in choline uptake in mitochondria, which is the rate-limiting step in S-adenosylmethionine (SAM) synthesis and DNA methylation. Identification of this CTL1- and CTL2-mediated choline transport system provides a potential new target for esophageal cancer therapy.

**Key Words:** Choline, Transporter, Esophageal cancer, Apoptotic cell death, Caspase-3/7

## INTRODUCTION

The incidence and mortality of esophageal cancer rank eighth and sixth, respectively, among common malignancies worldwide (Zhang, 2013). Risk factors for esophageal cancer include drinking alcohol and smoking (Xu, 2009). Indeed, people who drink and smoke are 30 times more likely to develop esophageal cancer than those who do not have these habits. The most common sites of esophageal cancer are the middle intrathoracic esophagus (about 50%), lower intrathoracic esophagus (about 25%), upper intrathoracic esophagus (about 15%), and cervical esophagus (about 5%) (Tachimori *et al.*, 2016). While the histologic type is mainly squamous cell carcinoma, the incidence of adenocarcinoma that is caused by reflux esophagitis is increasing (Tachimori *et al.*, 2016). Therapy for esophageal cancer includes surgical treatment,

chemotherapy and radiotherapy. Recently, however, the treatment outcome with surgery has plateaued. Thus, multimodal therapy that combines chemotherapy and radiotherapy is necessary to improve the treatment outcome. Therefore, the target molecule in novel esophageal cancer therapy needs to be identified.

Choline is a quaternary amine that is essential for all cells. It is used as a precursor of both the neurotransmitter acetylcholine and S-adenosylmethionine (SAM), a methyl donor, and is needed for the synthesis of the major membrane phospholipids phosphatidylcholine (PC) and sphingomyelin (Michel and Bakovic, 2012). Choline affects the expression of genes involved in cell proliferation, differentiation, and apoptosis in both normal cells and cancer cells. In addition, choline uptake is the rate-limiting step in cell proliferation and differentiation (Inazu, 2014). Tumors, including esophageal tumors, are

**Open Access** <https://doi.org/10.4062/biomolther.2017.113>

This is an Open Access article distributed under the terms of the Creative Commons Attribution Non-Commercial License (<http://creativecommons.org/licenses/by-nc/4.0/>) which permits unrestricted non-commercial use, distribution, and reproduction in any medium, provided the original work is properly cited.

Received May 30, 2017 Revised Jul 6, 2017 Accepted Jul 28, 2017

Published Online Dec 8, 2017

**\*Corresponding Author**

E-mail: inazu@tokyo-med.ac.jp

Tel: +81-3-3351-6141, Fax: +81-3-3351-6166

characterized by increased cell membrane synthesis. Since tumor cells require a large amount of choline, we can assume that esophageal tumors show a higher uptake of choline than the surrounding esophageal normal tissue. The study of choline transport and the characteristics of choline transporters is important if we wish to understand the mechanism that underlies membrane synthesis and cell signaling.

The role of positron emission tomography (PET) is rapidly expanding. In particular, choline PET and choline PET-computed tomography (CT) are now commonly performed clinically (García *et al.*, 2014). Choline PET has been shown to be highly effective for imaging several tumor types, including prostate carcinoma, brain tumor, lung metastasis from esophageal cancer, and mediastinal lymph node metastases. Choline PET can also be used to differentiate between malignant and benign lesions in various regions of the body, including the brain, head, bone, and soft tissue (Tian *et al.*, 2004). With regard to esophageal cancer, choline PET may enable the early diagnosis of an unsuspected esophageal carcinoma (Bertagna *et al.*, 2014). Choline PET is more effective than 2-deoxy-2-[fluorine-18]fluoro-D-glucose (<sup>18</sup>F-FDG) PET for detecting very small metastases localized in the mediastinum (Liu *et al.*, 2002). Further, a recent *in vitro* study suggested that choline PET might be a useful indicator of the response to chemotherapy agents that act by inhibiting signal transduction (Gillies and Morse, 2005). Previous studies have demonstrated abnormalities in choline uptake and choline phospholipid metabolism in cancer cells based on imaging by magnetic resonance spectroscopy (MRS) (Eliyahu *et al.*, 2007; Glunde *et al.*, 2011). The aberrant choline metabolism in cancer cells is strongly correlated with the progression of malignancy (Glunde *et al.*, 2006). Thus, choline uptake through choline transporters is both the rate-limiting step in choline phospholipid metabolism, and a prerequisite for cancer cell proliferation. However, the uptake of choline and the functional expression of choline transporters in human cancer including esophageal cancer are poorly understood.

The choline transport system has been categorized into three transporter families: high-affinity choline transporter 1 (CHT1), choline transporter-like proteins (CTLs), and poly-specific organic cation transporters (OCTs). CHT1 is a Na<sup>+</sup>-dependent that is thought to play a role in cholinergic neurons. The function of CHT1 is highly sensitive to the choline uptake inhibitor, hemicholinium-3 (HC-3). The CTL family consist of five genes, CTL1-5, and CTL1 is the predominant member of this family. CTL1 is Na<sup>+</sup>-independent, and is inhibited by a high concentration of HC-3 (Michel and Bakovic, 2012; Inazu, 2014). CTL1 and CTL2 are functionally expressed as choline transporters (Kommareddi *et al.*, 2010; Michel and Bakovic, 2012). Little is known about other transporters in this family. The OCT family consists of three genes, OCT1-3, which function through a Na<sup>+</sup>-independent uptake mechanism. OCT1 and OCT2 accept choline as a substrate with low affinity. However, OCT3 does not recognize choline as a substrate.

Thus, choline and the choline transport system are indispensable for all cells, including cancer cells. However, to date, little is known about the uptake system for choline and the functional expression of choline transporters in esophageal cancer. In this study, we performed a molecular and functional characterization of choline uptake in the esophageal cancer cells.

## MATERIALS AND METHODS

### Materials

The human esophageal cell lines (KYSE series) (Shimada *et al.*, 1992) were purchased from JCRB Cell Bank (Osaka, Japan). Human esophageal epithelial cells (HEEpiC) was purchased from ScienCell Research Laboratories, Inc (Carlsbad, CA, USA). [<sup>3</sup>H]Choline chloride (specific activity: 3182 GBq/mmol) and ATPLite™ were obtained from PerkinElmer Life Sciences, Inc (Boston, MA, USA). Diphenhydramine hydrochloride, triprolidine hydrochloride, alimemazine tartrate, hydroxyzine dihydrochloride, ketotifen fumarate, azelastine hydrochloride and ebastine were obtained from Funakoshi Co., Ltd (Osaka, Japan). Choline chloride, D-MEM, RPMI 1640, clemastine fumarate, chlorpheniramine maleate, mequitazine, oxatomide and bepotastine besilate were obtained from Wako Pure Chemical Industries, Ltd (Osaka, Japan). Promethazine hydrochloride, emedastine fumarate, epinastine hydrochloride, cetirizine dihydrochloride, loratadine, levocetirizine dihydrochloride, tranilast, suplatast tosilate, sodium cromoglicate and fexofenadine hydrochloride were obtained from Tokyo Chemical Industry Co., Ltd (Tokyo, Japan). Hemicholinium-3 (HC-3), N-methyl-D-glucamine (NMDG), TritonX-100, paroxetine hydrochloride, imipramine hydrochloride, propofol, homochlorcyclizine, quinidine hydrochloride, furosemide, rebamipide hydrate, mebendazole, acyclovir, amantadine hydrochloride, pirenzepine dihydrochloride, bepridil hydrochloride, lomeridine hydrochloride, urapidil hydrochloride, trazodone hydrochloride and cyproheptadine were obtained from Sigma-Aldrich Co. LLC (St. Louis, MO, USA). Alexa Fluor 568 goat anti-rabbit IgG was purchased from Molecular Probes Inc (Eugene, OR, USA). Tris-SDS β-ME sample solution and rupaadine were obtained from Cosmo Bio Corporation (Tokyo, Japan). D-MEM without choline chloride was obtained from Cell Science & Technology Institute, Inc (Miyagi, Japan). Citalopram hydrobromide and fluoxetine hydrochloride were purchased from LKT Laboratories, Inc (St. Paul, MN, USA). Fluvoxamine maleate, milnacipran hydrochloride and venlafaxine were obtained from Meiji Yakuin Co., Ltd (Tokyo, Japan), Asahi Kasei Pharma Corporation (Tokyo, Japan) and Wyeth-Ayerst Research (Princeton, NJ, USA), respectively. Dexmedetomidine hydrochloride was obtained from Maruishi Pharmaceutical Co. Ltd (Osaka, Japan). Reboxetine mesylate was purchased from Cayman Chemical Company (MI, USA). Caspase-Glo® 3/7 Assay was purchased from Promega Corporation (Madison, WI, USA). A TaqMan® RNA-to-CT™ 1-Step Kit and TaqMan® Gene Expression Assays were obtained from Applied Biosystems (Foster City, CA, USA). RIPA Lysis Buffer System was purchased from Santa Cruz Biotechnology, Inc (Santa Cruz, CA, USA). Horseradish peroxidase-conjugated anti-rabbit and anti-mouse IgG were purchased from Kirkegaard and Perry Laboratories Inc (Gaithersburg, MD, USA). A Protease Inhibitor Cocktail kit was purchased from Pierce Biotechnology (Rockford, IL, USA). Protein Multicolor was purchased from BioDynamics Laboratory Inc (Tokyo, Japan). 10% Mini-PROTEAN® TGX™ Gel and Trans-Blot™ Turbo™ Transfer Pack were purchased from Bio-Rad Laboratories, Inc (Tokyo, Japan). iBind™ Western Systems was purchased from ThermoFisher Scientific Inc (Waltham, MA, USA). Anti-CTL1 polyclonal antibody (ab110767), anti-COX IV polyclonal antibody (ab16056) and anti-Na<sup>+</sup>/K<sup>+</sup>-ATPase mouse monoclonal antibody (ab7671) were purchased from Abcam plc (Cam-

**Table 1.** Human squamous cell carcinoma cell line established from esophageal cancer (KYSE series)

Cell Name	Sex	Age	Stage	Profile
KYSE-180	Male	53	T4N1M0 Stage 3	Well differentiated squamous cell carcinoma
KYSE-450	Male	59	T1M1N0 stage 2b	Well differentiated squamous cell carcinoma
KYSE-510	Female	67	T4M1N0 stage 3	Well differentiated squamous cell carcinoma
KYSE-590	Male	39	T4M1N1 stage 4	Well differentiated squamous cell carcinoma
KYSE-790	Male	68	T4M1N1 stage 4	Well differentiated squamous cell carcinoma

bridge, UK). Anti-CTL2 monoclonal antibody (clone 3D11) was purchased from Abnova Corporation (Taipei City, Taiwan). Amersham™ ECL™ prime Western Blotting Detection reagent was purchased from GE Healthcare Life Sciences (Buckinghamshire, UK).

### Cell culture

Table 1 shows a profile of the human esophageal tumor cell line KYSE series. Cells were grown in RPMI 1640 medium supplemented with 10% fetal bovine serum (Gibco, Gaithersburg, MD, USA) and 20 mg/L kanamycin (Gibco) in non-coated flasks and 24-well plates. Cultures were maintained in a humidified atmosphere of 5% CO<sub>2</sub> and 95% air at 37°C, and the medium was changed every 3–4 days. In the experiments on the effects of choline deficiency (CD), cells were seeded at 1×10<sup>4</sup> cells/ml/well on 24-well culture plates and incubated in defined medium D-MEM with 30 μM choline chloride (Control) or without choline chloride (choline deficiency: CD). Cells were used for experiments after 2 days.

### RNA extraction and real-time polymerase chain reaction (PCR) assay

Total RNA was extracted from the cells using QIA shredder and an RNeasy Mini Kit according to the manufacturer's instructions. The TaqMan probes for the target mRNAs (CHT1, OCT1-3, CTL1-5 and the housekeeping gene glyceraldehyde-3-phosphate dehydrogenase (GAPDH)) were designed based on the human mRNA sequence using TaqMan® Gene Expression Assays. For one-step real-time PCR, 20 ng of total RNA was added to a master mixture by using the TaqMan® RNA-to-CT™ 1-Step Kit according to the manufacturer's instructions. Real-time PCR data were analyzed with the LightCycle® 96 system (Roche Diagnostics, Mannheim, Germany). The relative mRNA expression levels of the target genes in cells were calculated using the comparative cycle time (C<sub>t</sub>) method. The mRNA expression level relative to GAPDH for each target PCR can be calculated using the following equation: relative mRNA expression = 2<sup>-(C<sub>t</sub> target - C<sub>t</sub> GAPDH)</sup> × 100% (Inazu *et al.*, 2013).

### Western blot analysis

Cells were washed two times with D-PBS and were extracted on ice in a RIPA Lysis Buffer (2 mM PMSF, 1 mM sodium orthovanadate, protease inhibitor cocktail, 1mM EDTA, lysis buffer, pH 7.4), and then centrifuged (14,000 ×g) for 15 min at 4°C. The supernatant was incubated for 5 min at 100°C in a 1:1 (v:v) ratio of Tris-SDS β-ME sample solution and electrophoresed on 10% SDS gel with molecular weight standards. Proteins separated on 10% SDS-PAGE were transferred to PVDF membranes using by the Trans-Blot® Turbo™ Transfer System. After protein transfer, the membrane was blocked with iBind™ Flex Solution overnight at 4°C. Membranes were then

incubated with 1 μg/ml rabbit anti-CTL1 polyclonal antibody and 2 μg/ml anti-CTL2 monoclonal antibody in iBind™ Flex Solution and secondary antibody of anti-rabbit HRP (1 μg/ml) or anti-mouse HRP (1 μg/ml) using a iBind Flex Western Device for 2.5 h at room temperature. Protein bands were visualized using an ECL Prime Western Blotting Detection System (GE Healthcare Life Sciences, Marlborough, MA, USA). Luminescent images were obtained using a ChemiDoc XRS Plus System (Bio-Rad Laboratories, Hercules, CA, USA).

### Immunocytochemistry

Cells grown on a 35 mm Glass Base dish (IWAKI, Chiba, Japan) were washed twice with D-PBS and fixed with 100% methanol for 20 min at room temperature. Cells were permeabilized with detector blocking solution for CTL1 detection or iBind™ Flex Solution for CTL2 detection overnight at 4°C. Cells were incubated with anti-CTL1 polyclonal antibody (2 μg/ml), anti-CTL2 monoclonal antibody (2 μg/ml), anti-COX IV polyclonal antibody (2 μg/ml) and anti-Na<sup>+</sup>/K<sup>+</sup>-ATPase monoclonal antibody (5 μg/ml) in new blocking solution for 4 h at room temperature. After being washed with wash solution, the cells were incubated with 2 μg/ml Alexa Fluor 488 anti-rabbit IgG (Molecular Probes Inc.) and 2 μg/ml Alexa Fluor 568 anti-goat IgG for 1 h at room temperature. After excess antibody was washed out with wash solution, the specimens were mounted using VECTASHIELD mounting medium with DAPI (Vector Laboratories, Burlingame, CA, USA). Fluorescence images were obtained with a Confocal Laser Scanning Biological Microscope (FV10i-DOC, Olympus, Tokyo, Japan).

### [<sup>3</sup>H]Choline uptake into KYSE-180 cells

Cells were cultured in 24-well plates. The growth medium was removed from the 24-well plates, and cells were washed twice with uptake buffer, consisting of 125 mM NaCl, 4.8 mM KCl, 1.2 mM CaCl<sub>2</sub>, 1.2 mM KH<sub>2</sub>PO<sub>4</sub>, 5.6 mM glucose, 1.2 mM MgSO<sub>4</sub> and 25 mM HEPES adjusted to pH 7.4 with Tris. This was followed by the addition of [<sup>3</sup>H]choline. [<sup>3</sup>H]Choline uptake was terminated by removal of the uptake buffer and three rapid washes with ice-cold uptake buffer. Cells were dissolved in 0.1 M NaOH and 0.1% Triton X-100, and aliquots were taken for liquid scintillation counting and protein assay. The radioactivity was measured by a liquid scintillation counter (Tri-Carb® 2100TR, Packard, USA). When Na<sup>+</sup>-free buffer was used, the Na<sup>+</sup>-free buffer was modified by replacing NaCl with an equimolar concentration of N-methyl-D-glucamine chloride. Uptake buffers of varying pH (pH 6.0, 6.5, 7.0, 7.5, 8.0, and 8.5) were prepared by mixing 25 mM MES (pH 5.5) and 25 mM Tris (pH 8.5). Both buffers contained 125 mM NaCl, 4.8 mM KCl, 1.2 mM CaCl<sub>2</sub>, 1.2 mM KH<sub>2</sub>PO<sub>4</sub>, 5.6 mM glucose and 1.2 mM MgSO<sub>4</sub>. In the experiment on saturation kinetics, the concentration of [<sup>3</sup>H]choline was kept constant at 10 nM and

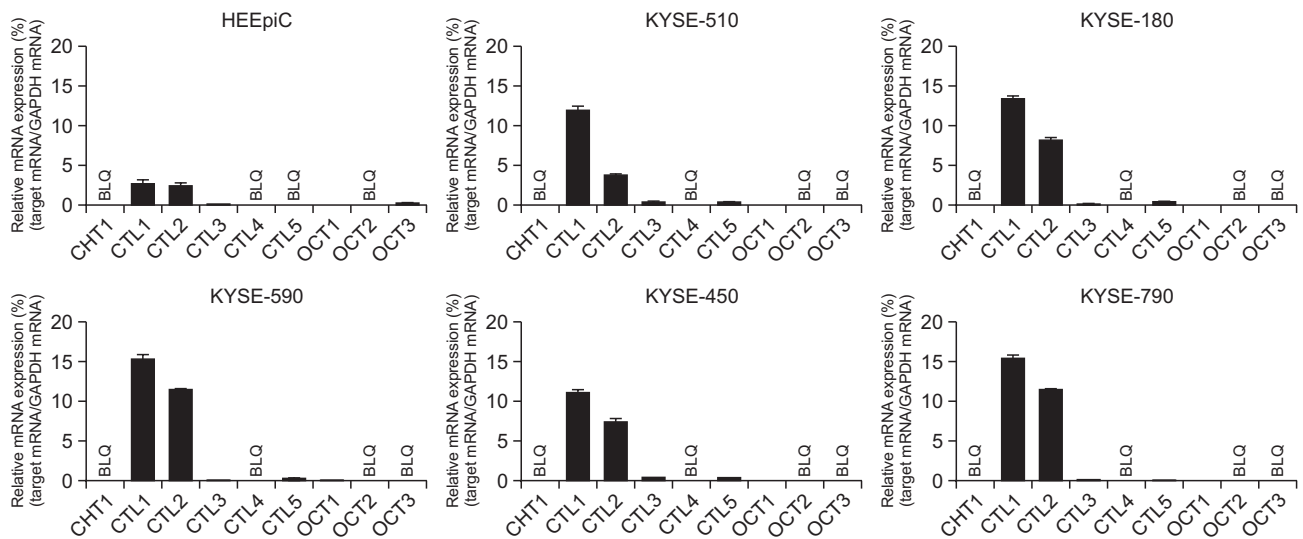


**Fig. 1.** Expression of mRNA for choline transporters in HEEpiC and KYSE cells. Real-time PCR analysis of the expression of mRNAs for CHT1, CTL1-5, and OCT1-3. Relative mRNA expression is expressed as a ratio of the target mRNA to GAPDH mRNA. Experiments were performed in triplicate. Each column represents the mean  $\pm$  SD (n=3). BLQ means below the limit of quantification.

unlabeled choline was added to give the desired choline concentration. The specific uptake of [<sup>3</sup>H]choline was calculated as the difference between total [<sup>3</sup>H]choline uptake in the presence and absence of 30 mM unlabeled choline (Iwao *et al.*, 2016). Protein concentrations were determined using a DC Protein Assay Kit (Bio-Rad Laboratories, Hercules, CA, USA).

**Cell viability assay**

Cells were plated and cultured on 24-well plates. Inhibitors were added after 24 h of cell culture, and the final volume of medium in each well was 1.0 ml. Cell numbers were measured using an ATPLite™, and the luminescence ATP detection assay system was used as described in the manufacturer’s instructions. Luminescence was measured on a FilterMax F5 Multi-Mode Microplate Reader (Molecular Devices, LLC, Sunnyvale, CA, USA). The assay was linear over a large range of ATP concentrations (5×10<sup>-9</sup> to 10<sup>-6</sup> mol/L) and with a large variety of cell numbers in the assay. There is a linear correlation between the luminescence signal and the cell number (Nishiyama *et al.*, 2016).

**Measurements of the caspase-3/7 activity**

For measurements of the activities of caspase-3/7, the Caspase-Glo® 3/7 Assay was carried out according to the manufacturer’s instruction. This kit is based on the cleavage of the DEVD sequence of a luminogenic substrate by caspase-3/7, which results in a luminescent signal (Nishiyama *et al.*, 2016). KYSE-180 cells were seeded at a density of 1×10<sup>4</sup> cells/well in 24-well plates. Test drugs were added 24 h after cell plating, and the final volume of medium in each well was 1.0 ml. Luminescence was measured on a FilterMax F5 Multi-Mode Microplate Reader (Molecular Devices, LLC).

**Data analysis**

Data are expressed as mean  $\pm$  SD. Statistical analyses were performed with the unpaired *t*-test and Dunnett multiple comparisons test using commercially available software (Prism 6, GraphPad Software, Inc., San Diego, CA, USA). The

results were considered to be statistically significant when *p*-values were less than 0.05. The time courses of choline uptake were compared after fitting into single exponential decay equations. The kinetic parameters (*K<sub>m</sub>* and *V<sub>max</sub>*) and the half-inhibitory concentration (*IC<sub>50</sub>*) values were calculated by non-linear regression methods and Eadie-Hofstee curves were fitted using linear regression with the commercially available software Prism 6 (GraphPad Software, Inc.).

**RESULTS**

**Expression of choline transporters in human esophageal epithelial cells (HEEpiC) and esophageal cancer cell lines (KYSE series)**

The expression of mRNA for CHT1, CTL1-5 and OCT1-3 was investigated by real-time PCR analysis (Fig. 1). In the KYSE cell lines, CTL1 and CTL2 mRNA were highly expressed, while CHT1, CTL4, OCT2 and OCT3 mRNA were not expressed. CTL3, CTL5 and OCT1 mRNA were expressed at a low level. In contrast, the CTL1 and CTL2 mRNA expression in HEEpiC was lower than that of KYSE series. The expression patterns of the transporters closely resembled it in all KYSE series. Therefore, we conducted a molecular and functional analysis using KYSE-180 cells.

CTL1 and CTL2 mRNA were mainly expressed in KYSE cell lines and HEEpiC by real-time PCR analysis. Therefore, we examined the expression of CTL1 and CTL2 at the protein level. Extracts of KYSE-180 cell lysate were immunoblotted with anti-CTL1 and anti-CTL2 antibody. Immunoblot assays with CTL1 and CTL2 antibody demonstrated the presence of a band of 70 kDa, respectively, in KYSE 180 cells (Fig. 2A).

The subcellular distribution of CTL1 and CTL2 in KYSE-180 cells was determined by immunocytochemical staining (Fig. 2B). Immunocytochemical staining using anti-CTL1 antibody revealed that the cell surface showed immunoreactivity, and overlapped that of the plasma membrane marker Na<sup>+</sup>/K<sup>+</sup>-ATPase (Fig. 2C). On the other hand, CTL2 immunoreactivity



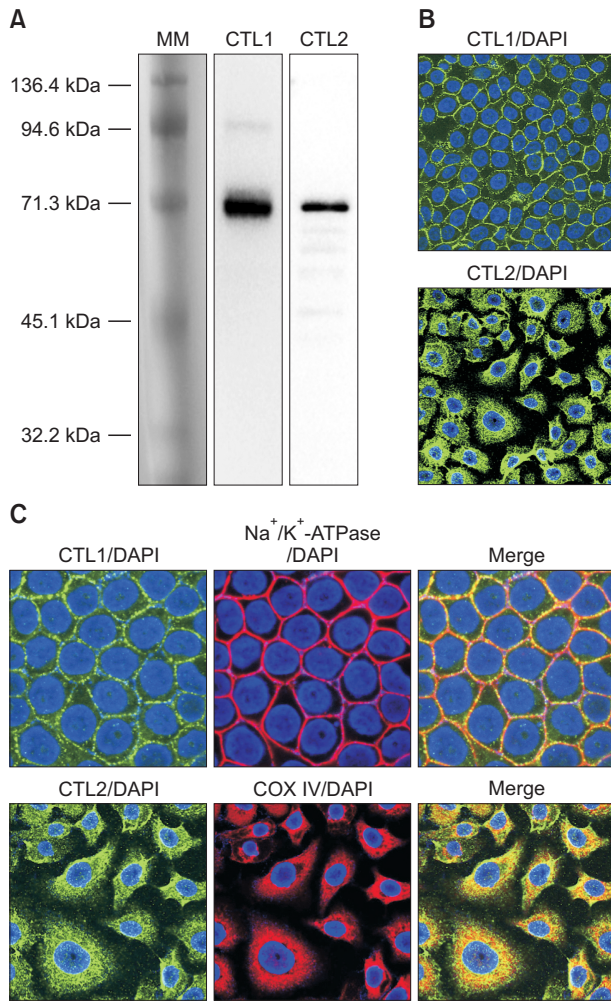


**Fig. 2.** Expression of protein for CTL1 and CTL2 in KYSE-180 cells. (A) Detection of CTL1 and CTL2 proteins by western blot analysis. MM, pre-stained protein molecular weight marker. (B) Subcellular distribution of CTL1 and CTL2 proteins by immunocytochemistry. (C) Fluorescence from antibodies directed to CTL1 (green), CTL2 (green), Na<sup>+</sup>/K<sup>+</sup>-ATPase (red) and COX IV (red) was imaged with a confocal microscope. Nuclei are stained with DAPI (blue). Merged images are shown in Merge, and yellow represents co-localization.

was recognized in intracellular compartments, and overlapped that of the mitochondrial marker COX IV (Fig. 2C).

### Time course and kinetics of [<sup>3</sup>H]choline uptake in KYSE 180 cells

We examined the time course of [<sup>3</sup>H]choline uptake in the presence and absence of extracellular Na<sup>+</sup> in KYSE 180 cells for 60 min (Fig. 3A). [<sup>3</sup>H]Choline uptake increased in a time-dependent manner; it was linear with time up to at least 20 min. When NaCl in the uptake buffer was replaced by NMDG-Cl, the uptake of [<sup>3</sup>H]choline uptake under Na<sup>+</sup>-free conditions was weakly decreased compared to control uptake under normal conditions. These uptake was not statistically significant, indicates that it is a Na<sup>+</sup>-independent transport system. The characteristics of the kinetics of [<sup>3</sup>H]choline uptake by KYSE 180 cells were determined (Fig. 3B). A kinetic analysis of [<sup>3</sup>H]

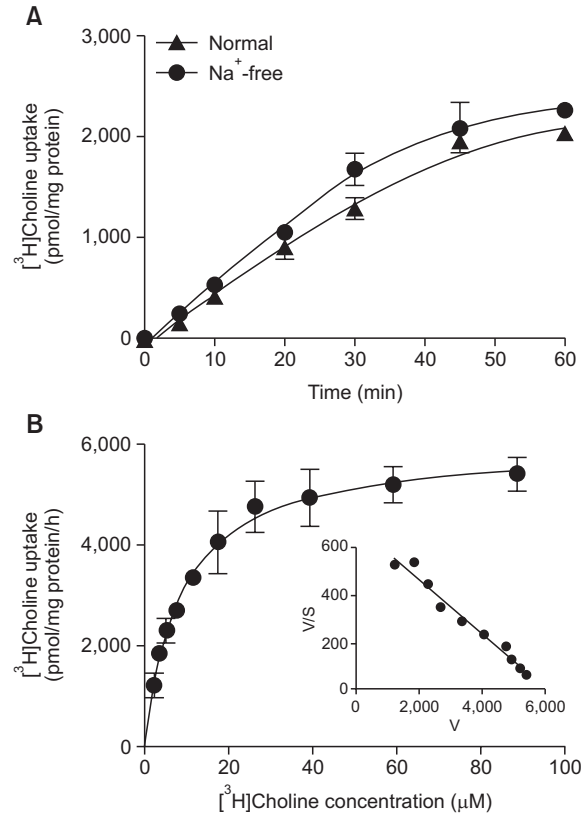


**Fig. 3.** Time course and Na<sup>+</sup>-dependence of [<sup>3</sup>H]choline uptake in KYSE-180 cells. (A) Time course of 10 μM [<sup>3</sup>H]choline uptake in the presence (▲) and absence (●) of extracellular Na<sup>+</sup> for 60 min. The time-course of [<sup>3</sup>H]choline uptake was fitted to the experimental data by a non-linear regression analysis. Each point represents the mean ± SD (n=4). (B) Kinetic characteristics of [<sup>3</sup>H]choline uptake in KYSE-180 cells. Cells were incubated for 20 min with [<sup>3</sup>H]choline at concentrations of 2.3 to 88.9 μM. Each point represents the mean ± SD (n=4). An analysis of the kinetics of [<sup>3</sup>H]choline uptake, as computed by a non-linear regression analysis, yielded a  $K_m$  value of  $8.6 \pm 0.8 \mu\text{M}$ , and a  $V_{max}$  value of  $6001.0 \pm 167.8 \text{ pmol/mg protein/h}$ . Inset: Eadie-Hofstee plots of [<sup>3</sup>H]choline uptake show single straight lines.

choline uptake (specific uptake), as computed by a nonlinear regression analysis, yielded a Michaelis-Menten constant ( $K_m$ ) of  $8.6 \pm 0.8 \mu\text{M}$  and a maximal velocity ( $V_{max}$ ) of  $6001.0 \pm 167.8 \text{ pmol/mg protein/h}$ . The Eadie-Hofstee plot shows a straight line in these cells. These data suggest that [<sup>3</sup>H]choline uptake into KYSE 180 cells is mediated by a single intermediate-affinity transport system.

### Properties of [<sup>3</sup>H]choline uptake in KYSE-180 cells

It has been reported that choline uptake through CTL1 is completely inhibited by HC-3 in the μM range (Inazu, 2014). We investigated the inhibitory effects of HC-3, a choline uptake inhibitor, on the uptake of [<sup>3</sup>H]choline into KYSE-180 cells (Fig. 4A). [<sup>3</sup>H]Choline uptake was inhibited by HC-3 in a concentration-dependent manner. The  $K_i$  value for the inhibition of [<sup>3</sup>H]choline uptake by HC-3 in KYSE-180 cells was 17.8 μM.

It has been reported that choline uptake through CTL1 is pH-dependent (Inazu, 2014). The influence of extracellular pH on the uptake of [<sup>3</sup>H]choline in KYSE-180 cells was exam-

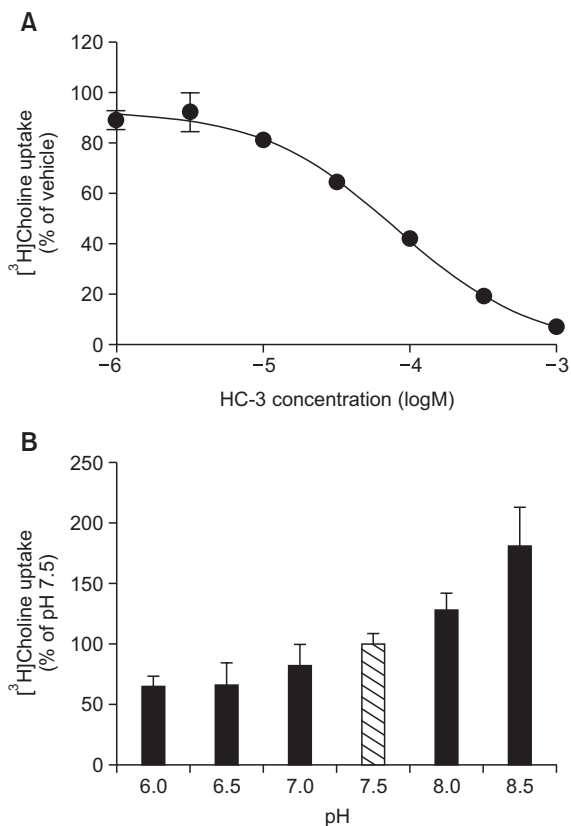


**Fig. 4.** Properties of [<sup>3</sup>H]choline uptake in KYSE-180 cells. (A) Effects of HC-3 on [<sup>3</sup>H]choline uptake in KYSE-180 cells. Cells were pre-incubated with various concentrations of HC-3 for 20 min, and the uptake of 10 μM [<sup>3</sup>H]choline was then measured for 20 min. Results are given as a percentage of the control uptake measured in the presence of vehicle. Each point represents the mean ± SD (n=4). (B) Influence of extracellular pH on [<sup>3</sup>H]choline uptake in KYSE-180 cells. The uptake of 10 μM [<sup>3</sup>H]choline was measured for 20 min under different pH conditions. The results show [<sup>3</sup>H]choline uptake as a percentage of that at pH 7.5. Each column represents the mean ± SD (n=4).

ined by varying the pH of the pre-incubation and incubation media between pH 6.0 and 8.5 (Fig. 4B). [<sup>3</sup>H]Choline uptake decreased when the extracellular pH was changed from 7.5 to 6.0, and was increased when the pH of the extracellular medium was changed from 7.5 to 8.5.

**Influence of choline deficiency on cell viability and caspase-3/7 activity in KYSE-180 cells**

We investigated the influence of choline deficiency on cell viability and caspase-3/7 activity in KYSE-180 cells (Fig. 5). Cells were seeded at 1×10<sup>4</sup> cells/ml/well on 24-well culture plates and incubated in defined medium D-MEM with 30 μM choline chloride (control) or without choline chloride (choline deficiency: CD) for 2 days. Choline deficiency significantly inhibited cell viability and significantly increased caspase-3/7 activity in KYSE-180 cells.

**Effects of various drugs on [<sup>3</sup>H]choline uptake and cell viability in KYSE-180 cells**

We examined the inhibitory effects of 47 various drugs (100 μM) on [<sup>3</sup>H]choline uptake and cell viability in KYSE-

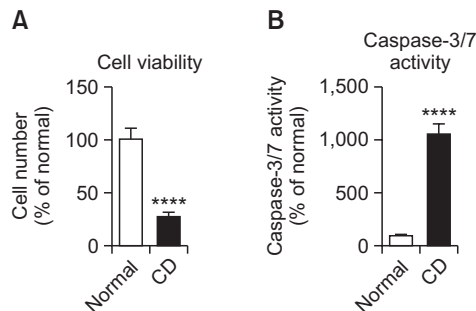


**Fig. 5.** Influence of choline deficiency on cell viability (A) and caspase-3/7 activity (B) in KYSE-180 cells. Cells were seeded at 1×10<sup>4</sup> cells/well on 24-well culture plates and incubated in defined medium D-MEM with 4 mg/L choline chloride (Normal) or without choline chloride (choline deficiency: CD) for 2 days. Cell numbers and caspase-3/7 activity were then measured. Each column represents the mean ± SD (n=4). \*\*\*\*p<0.0001 compared with the normal conditions.

180 cells (Fig. 6). Several cationic drugs inhibited [<sup>3</sup>H]choline uptake (Fig. 6A) and cell viability (Fig. 6B). The correlations between the effects of 47 various drugs on [<sup>3</sup>H]choline uptake and cell viability were significant (r=0.64, p<0.0001) (Fig. 6C). We examined the effects of 7 cationic drugs (bepidil, rupatadine, paroxetine, mequitazine, loratadine, clemastine and azelastine, which are surrounded by a circle in Fig. 6C) on caspase-3/7 activity, which inhibited both cell viability, and [<sup>3</sup>H]choline uptake. These drugs can inhibit cell viability, and increased caspase-3/7 activity in KYSE-180 cells (Fig. 7).

**DISCUSSION**

Choline PET and MRS have shown that enhanced choline transport may play a role in the elevation of phosphocholine (PCho) levels in cancer cells (Ackerstaff *et al.*, 2003; Eliyahu *et al.*, 2007). The elevation of PCho and total choline is one of the most widely established characteristics of cancer cells. PCho is a precursor and a breakdown product of PC, the most abundant phospholipid in biological membranes. The intracellular accumulation of choline through choline transporters is the rate-limiting step in choline phospholipid metabolism, and a prerequisite for cancer cell proliferation. It is important that we characterize the underlying mechanism and the expression of choline transport systems in cancer cells.

We first examined the expression of mRNA for CHT1, CTL1-5 and OCT1-3 in HEEpIC and KYSE cells by real-time RT-PCR analysis. We found that CTL1 and CTL2 mRNA were mainly expressed in all KYSE cells, and these expression levels are higher than HEEpIC. Furthermore, both CTL1 and CTL2 proteins were expressed, and were localized in the plasma membrane and mitochondria, respectively. These results indicate that CTL1 may be involved in the uptake of extracellular choline into cancer cells. KYSE-180 cells have a Na<sup>+</sup>-independent and an intermediate-choline transport systems that can be characterized by kinetic parameters and Eadie-Hofstee plots. The K<sub>m</sub> value was 8.6 μM, which is similar to those in the human cell line, and these cell types show properties similar to those of CTL1. CTL1 is known to be pH-dependent, and can be completely inhibited by HC-3 in the μM range (Inazu *et al.*,

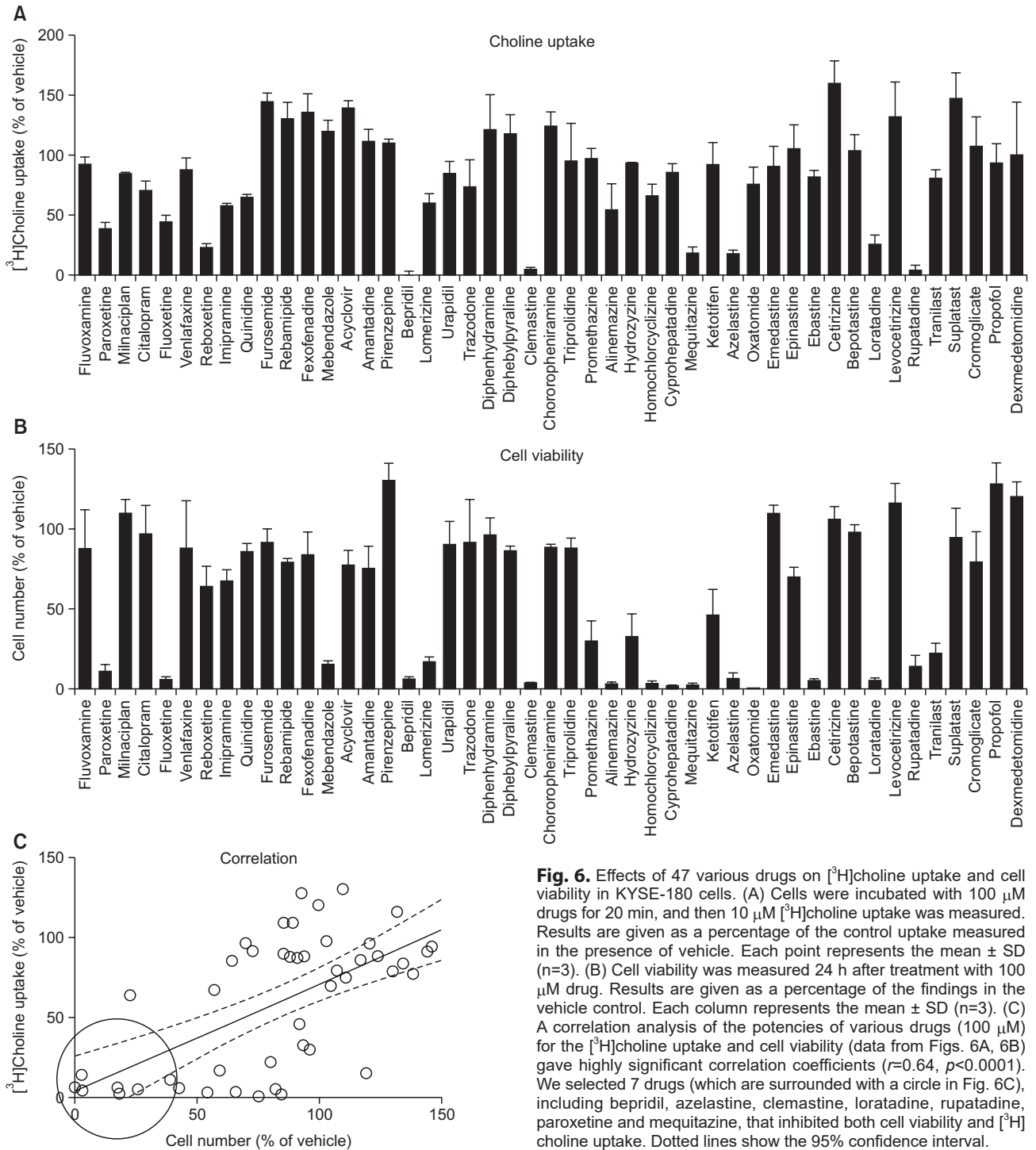


**Fig. 6.** Effects of 47 various drugs on  $[^3\text{H}]$ choline uptake and cell viability in KYSE-180 cells. (A) Cells were incubated with 100  $\mu\text{M}$  drugs for 20 min, and then 10  $\mu\text{M}$   $[^3\text{H}]$ choline uptake was measured. Results are given as a percentage of the control uptake measured in the presence of vehicle. Each point represents the mean  $\pm$  SD ( $n=3$ ). (B) Cell viability was measured 24 h after treatment with 100  $\mu\text{M}$  drug. Results are given as a percentage of the findings in the vehicle control. Each column represents the mean  $\pm$  SD ( $n=3$ ). (C) A correlation analysis of the potencies of various drugs (100  $\mu\text{M}$ ) for the  $[^3\text{H}]$ choline uptake and cell viability (data from Figs. 6A, 6B) gave highly significant correlation coefficients ( $r=0.64$ ,  $p<0.0001$ ). We selected 7 drugs (which are surrounded with a circle in Fig. 6C), including bepridil, azelastine, clemastine, loratadine, rupatadine, paroxetine and mequitazine, that inhibited both cell viability and  $[^3\text{H}]$  choline uptake. Dotted lines show the 95% confidence interval.

2005). In this study,  $[^3\text{H}]$ choline uptake in KYSE-180 cells was decreased by acidification and increased by alkalization of the extracellular medium, indicating that choline may be transported by a choline/ $\text{H}^+$  antiport system. Moreover, the  $K_i$  value of HC-3 for KYSE-180 cells is 17.8  $\mu\text{M}$ , which is very close to the  $K_i$  value for CTL1. These results suggest that  $[^3\text{H}]$ choline uptake in KYSE-180 cells is likely mediated by CTL1. Therefore, intermediate-affinity choline uptake via CTL1 is believed

to play an important role in choline transport in esophageal cancer. The presence of CTL1-mediated choline uptake has been suggested in primary cultures of rat astrocytes (Inazu *et al.*, 2005), mouse neurons (Fujita *et al.*, 2006), human keratinocytes (Uchida *et al.*, 2009), human colon carcinoma cells (Kouji *et al.*, 2009), rat renal tubule epithelial cells (Yabuki *et al.*, 2009), human neuroblastoma cells (Yamada *et al.*, 2011) and small cell lung carcinoma cells (Inazu *et al.*, 2013). CTL1

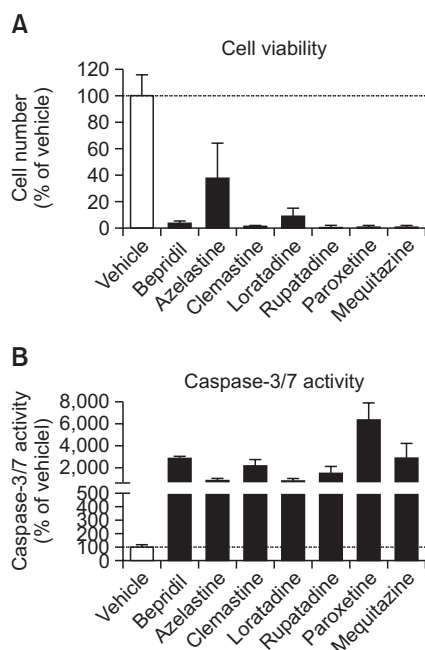


**Fig. 7.** Effects of 7 drugs that inhibited both cell viability and [ $^3\text{H}$ ] choline uptake on cell viability (A) and caspase-3/7 activity (B) in KYSE-180 cells. Cells were incubated with 100  $\mu\text{M}$  cationic drugs for 8 h. Cell numbers and caspase-3/7 activity were then measured. Results are given as a percentage of the findings in the vehicle control. Each column represents the mean  $\pm$  SD (n=4).

is ubiquitously expressed in mammalian tissues which suggests that it plays an important role in choline transporter for a broader purpose, such as ACh, PCho and phospholipid synthesis. CTL1 is strongly expressed in cancer cells such as breast cancer (Eliyahu *et al.*, 2007) and lung adenocarcinoma (Wang *et al.*, 2007), which require high levels of choline to synthesize sphingomyelin, PCho and PC.

We investigated the relationship between apoptotic cell death and the inhibition of intracellular choline uptake in KYSE-180 cells. We found that choline deficiency significantly inhibited cell viability and significantly increased caspase-3/7 activity. We concluded that the choline deficiency in KYSE-180 cells caused apoptotic cell death. These results demonstrate that the functional inhibition of choline uptake through CTL1 could promote apoptotic cell death. Many studies have reported that various organic cations inhibited choline uptake and cell viability (Kouji *et al.*, 2009; Yamada *et al.*, 2011; Nishiyama *et al.*, 2016). A correlation analysis of the potencies of organic cations for the inhibition of choline uptake and cell viability showed a strong correlation in tongue cancer HSC-3 cells (Nishiyama *et al.*, 2016). Thus, these results indicate that there is a strong correlation between cell survival and the inhibition of choline uptake. In addition, HSC-3 cells cultured with choline-deficiency medium that were stained with FITC-annexin V, which indicates that they were apoptotic cells (Nishiyama *et al.*, 2016). These results demonstrate that the functional inhibition of CTL1 could promote apoptotic cell death. We explored the possible correlation between choline uptake and cell viability by examining the effects of 47 various drugs on the survival of KYSE-180 cells. We found a strong correlation between cell survival and the inhibition of cho-

line uptake ( $r=0.64$ ,  $p<0.0001$ ). Furthermore, choline uptake inhibitors can inhibit cell viability and increase caspase-3/7 activity. It may be possible to induce apoptotic cell death by obstructing the function of choline uptake through CTL1 in KYSE-180 cells. In the near future, it is necessary to evaluate these drugs in vivo tumor xenograft experiments using KYSE-180 cells. These choline uptake inhibitors induced changes in total choline uptake could affect PET tumor imaging, and it may be available as a PET tracer. Previous studies have shown that choline deficiency triggers apoptosis via a p53-independent pathway (Albright *et al.*, 1996) and increases the amount of ceramide, a lethal metabolite, in PC12 cells and primary neurons (Yen *et al.*, 1999). An increase in ceramide was associated with choline deficiency-induced apoptosis. The inhibition of choline transport decreased PCho and PC contents; cancer cells attempt to overcome this by activating an alternative mechanism for generating PCho and PC. This enables cancer cells, to some extent, to continue PCho and PC production, but also leads to the production of ceramide by the sphingomyelinase-catalyzed hydrolysis of sphingomyelin. Caspase-3 is activated following the induction of ceramide accumulation, and could promote apoptotic cell death.

The physiological function of CTL2 is not well understood. However, there have been some reports on this subject. CTL2 mRNA and protein are expressed in the human inner ear (Nair *et al.*, 2004), rat renal epithelial cells (Yabuki *et al.*, 2009), human trophoblastic cells (Yara *et al.*, 2015), human glioblastoma cells (Taguchi *et al.*, 2014), human brain microvascular endothelial cells (Iwao *et al.*, 2016) and human tongue cancer cells (Nishiyama *et al.*, 2016). The intracellular localization of CTL2 differs among these cells and it is located in the plasma membrane and mitochondria. It has recently been demonstrated that CTL2 exhibits detectable choline transport activity (Kommareddi *et al.*, 2010). However, the function of CTL2 has not been fully characterized and  $K_m$  values for choline are unknown. We found that CTL2 mRNA and protein were mainly expressed in KYSE-180 cells and CTL2 protein was located in mitochondria. SAM act as a major source of methyl groups and play an essential role as an epigenetics. The main intracellular source of SAM is from the oxidation of choline in mitochondria. Choline oxidase is located in the inner membrane of mitochondria in liver and kidney (Porter *et al.*, 1992; Kaplan *et al.*, 1993; O'Donoghue *et al.*, 2009), which shows that intracellular choline must cross the mitochondrial inner membrane before oxidation can occur. Interestingly, choline deficiency causes mitochondrial and cellular oxidative damage and lipid peroxidation (Ossani *et al.*, 2007). Thus, choline is also an essential substance for mitochondria. We found that the apoptotic cell death was induced by choline deficiency in KYSE cells. We speculate that CTL2 might be the major site for the control of choline oxidation in mitochondria and may be important molecules of the apoptotic cell death in esophageal cancer cells. Chemical modifications of histones and DNA, such as histone methylation, histone acetylation, and DNA methylation, play critical roles in epigenetic gene regulation (Kaelin and McKnight, 2013). SAM contains the active methyl donor group that is used by most methyltransferase enzymes. Altered DNA methylation and disruption of DNA repair have been reported in cancer patients (Balassiano *et al.*, 2011). Therefore, epigenetic mechanisms play important roles in carcinogenesis. Further studies will be needed to examine the function of CTL2 and its association with epigenetics in



esophageal cancer cells.

We conclude that KYSE-180 cells express the intermediate-affinity choline transporter CTL1, which uses a directed H<sup>+</sup> gradient as a driving force. Choline uptake through CTL1 is associated with cell viability, and the functional inhibition of CTL1 could promote apoptotic cell death. Furthermore, CTL2 may be involved in choline uptake in mitochondria, which is the rate-limiting step in SAM synthesis and DNA methylation. Identification of this CTL1- and CTL2-mediated choline transport system should provide a potential new target for esophageal cancer therapy.

## CONFLICT OF INTEREST

The authors have declared that there is no conflict of interest.

## ACKNOWLEDGMENTS

This work was supported by JSPS KAKENHI Grant Number 17K08315.

## REFERENCES

- Ackerstaff, E., Glunde, K. and Bhujwalla, Z. M. (2003) Choline phospholipid metabolism: a target in cancer cells? *J. Cell. Biochem.* **90**, 525-533.
- Albright, C. D., Liu, R., Bethea, T. C., Da Costa, K. A., Salganik, R. I. and Zeisel, S. H. (1996) Choline deficiency induces apoptosis in SV40-immortalized CWSV-1 rat hepatocytes in culture. *FASEB J.* **10**, 510-516.
- Balassiano, K., Lima, S., Jenab, M., Overvad, K., Tjonneland, A., Boutron-Ruault, M. C., Clavel-Chapelon, F., Canzian, F., Kaaks, R., Boeing, H., Meidtner, K., Trichopoulou, A., Laglou, P., Vineis, P., Panico, S., Palli, D., Grioni, S., Tumino, R., Lund, E., Bueno-de-Mesquita, H. B., Numans, M. E., Peeters, P. H., Ramon Quirós, J., Sánchez, M. J., Navarro, C., Ardanaz, E., Dorronsoro, M., Hallmans, G., Stenling, R., Ehrnström, R., Regner, S., Allen, N. E., Travis, R. C., Khaw, K. T., Offerhaus, G. J., Sala, N., Riboli, E., Hainaut, P., Scazecz, J. Y., Sylla, B. S., Gonzalez, C. A. and Herceg, Z. (2011) Aberrant DNA methylation of cancer-associated genes in gastric cancer in the European Prospective Investigation into Cancer and Nutrition (EPIC-EURGAST). *Cancer Lett.* **311**, 85-95.
- Bertagna, F., Bertoli, M., Treglia, G., Manenti, S., Salemme, M. and Giubbini, R. (2014) Incidental <sup>11</sup>C-Choline PET/CT uptake due to Esophageal carcinoma in a patient studied for prostate cancer. *Clin. Nucl. Med.* **39**, e442-e444.
- Eliyahu, G., Kreizman, T. and Degani, H. (2007) Phosphocholine as a biomarker of breast cancer: molecular and biochemical studies. *Int. J. Cancer* **120**, 1721-1730.
- Fujita, T., Shimada, A., Okada, N. and Yamamoto, A. (2006) Functional characterization of Na<sup>+</sup>-independent choline transport in primary cultures of neurons from mouse cerebral cortex. *Neurosci. Lett.* **393**, 216-221.
- García, J. R., Ponce, A., Canales, M., Ayuso, J., Moragas, M. and Soler, M. (2014) Detection of second tumors in <sup>11</sup>C-choline PET/CT studies performed due to biochemical recurrence of prostate cancer. *Rev. Esp. Med. Nucl. Imagen Mol.* **33**, 28-31.
- Gillies, R. J. and Morse, D. L. (2005) *In vivo* magnetic resonance spectroscopy in cancer. *Annu. Rev. Biomed. Eng.* **7**, 287-326.
- Glunde, K., Jiang, L., Moestue, S. A. and Gribbestad, I. S. (2011) MRS and MRSI guidance in molecular medicine: targeting and monitoring of choline and glucose metabolism in cancer. *NMR Biomed.* **24**, 673-690.
- Glunde, K., Jacobs, M. A. and Bhujwalla, Z. M. (2006) Choline metabolism in cancer: implications for diagnosis and therapy. *Expert Rev. Mol. Diagn.* **6**, 821-829.
- Inazu, M. (2014) Choline transporter-like proteins CTLs/SLC44 family as a novel molecular target for cancer therapy. *Biopharm. Drug Dispos.* **35**, 431-449.
- Inazu, M., Takeda, H. and Matsumiya, T. (2005) Molecular and functional characterization of a Na<sup>+</sup>-independent choline transporter in rat astrocytes. *J. Neurochem.* **94**, 1427-1437.
- Inazu, M., Yamada, T., Kubota, N. and Yamanaka, T. (2013) Functional expression of choline transporter-like protein 1 (CTL1) in small cell lung carcinoma cells: a target molecule for lung cancer therapy. *Pharmacol. Res.* **76**, 119-131.
- Iwao, B., Yara, M., Hara, N., Kawai, Y., Yamanaka, T., Nishihara, H., Inoue, T. and Inazu, M. (2016) Functional expression of choline transporter like-protein 1 (CTL1) and CTL2 in human brain microvascular endothelial cells. *Neurochem. Int.* **93**, 40-50.
- Kaelin, W. G., Jr. and McKnight, S. L. (2013) Influence of metabolism on epigenetics and disease. *Cell* **153**, 56-69.
- Kaplan, C. P., Porter, R. K. and Brand, M. D. (1993) The choline transporter is the major site of control of choline oxidation in isolated rat liver mitochondria. *FEBS Lett.* **321**, 24-26.
- Kommareddi, P. K., Nair, T. S., Thang, L. V., Galano, M. N., Babu, E., Ganapathy, V., Kanazawa, T., McHugh, J. B. and Carey, T. E. (2010) Isoforms, expression, glycosylation, and tissue distribution of CTL2/SLC44A2. *Protein J.* **29**, 417-426.
- Kouji, H., Inazu, M., Yamada, T., Tajima, H., Aoki, T. and Matsumiya, T. (2009) Molecular and functional characterization of choline transporter in human colon carcinoma HT-29 cells. *Arch. Biochem. Biophys.* **483**, 90-98.
- Liu, D., Hutchinson, O. C., Osman, S., Price, P., Workman, P. and Aboagye, E. O. (2002) Use of radiolabelled choline as a pharmacodynamic marker for the signal transduction inhibitor geldanamycin. *Br. J. Cancer* **87**, 783-789.
- Michel, V. and Bakovic, M. (2012) The ubiquitous choline transporter SLC44A1. *Cent. Nerv. Syst. Agents Med. Chem.* **12**, 70-81.
- Nair, T. S., Kozma, K. E., Hoefling, N. L., Kommareddi, P. K., Ueda, Y., Gong, T. W., Lomax, M. I., Lansford, C. D., Telian, S. A., Satar, B., Arts, H. A., El-Kashlan, H. K., Berryhill, W. E., Raphael, Y. and Carey, T. E. (2004) Identification and characterization of choline transporter-like protein 2, an inner ear glycoprotein of 68 and 72 kDa that is the target of antibody-induced hearing loss. *J. Neurosci.* **24**, 1772-1779.
- Nishiyama, R., Nagashima, F., Iwao, B., Kawai, Y., Inoue, K., Midori, A., Yamanaka, T., Uchino, H. and Inazu, M. (2016) Identification and functional analysis of choline transporter in tongue cancer: A novel molecular target for tongue cancer therapy. *J. Pharmacol. Sci.* **131**, 101-109.
- O'Donoghue, N., Sweeney, T., Donagh, R., Clarke, K. J. and Porter, R. K. (2009) Control of choline oxidation in rat kidney mitochondria. *Biochim. Biophys. Acta* **1787**, 1135-1139.
- Ossani, G., Dalghi, M. and Repetto, M. (2007) Oxidative damage lipid peroxidation in the kidney of choline-deficient rats. *Front. Biosci.* **12**, 1174-1183.
- Porter, R. K., Scott, J. M. and Brand, M. D. (1992) Choline transport into rat liver mitochondria. Characterization and kinetics of a specific transporter. *J. Biol. Chem.* **267**, 14637-14646.
- Shimada, Y., Imamura, M., Wagata, T., Yamaguchi, N. and Tobe, T. (1992) Characterization of 21 newly established esophageal cancer cell lines. *Cancer* **69**, 277-284.
- Tachimori, Y., Ozawa, S., Numasaki, H., Fujishiro, M., Matsubara, H., Oyama, T., Shinoda, M., Toh, Y., Udagawa, H. and Uno, T. (2016) Comprehensive registry of esophageal cancer in Japan, 2009. *Esophagus* **13**, 110-137.
- Taguchi, C., Inazu, M., Saiki, I., Yara, M., Hara, N., Yamanaka, T. and Uchino, H. (2014) Functional analysis of [methyl-<sup>3</sup>H]choline uptake in glioblastoma cells: influence of anti-cancer and central nervous system drugs. *Biochemical. Pharmacol.* **88**, 303-312.
- Tian, M., Zhang, H., Oriuchi, T., Higuchi, T. and Endo, K. (2004) Comparison of <sup>11</sup>C-choline PET and FDG PET for the differential diagnosis of malignant tumors. *Eur. J. Nucl. Med. Mol. Imaging* **31**, 1064-1072.
- Uchida, Y., Inazu, M., Takeda, H., Yamada, T., Tajima, H. and Matsumiya, T. (2009) Expression and functional characterization of

- choline transporter in human keratinocytes. *J. Pharmacol. Sci.* **109**, 102-109.
- Wang, T., Li, J., Chen, F., Zhao, Y., He, X., Wan, D. and Gu, J. (2007) Choline transporters in human lung adenocarcinoma: expression and functional implications. *Acta Biochim. Biophys. Sin. (Shanghai)* **39**, 668-674.
- Xu, X. C. (2009) Risk factors and gene expression in esophageal cancer. *Methods Mol. Biol.* **471**, 335-360.
- Yabuki, M., Inazu, M., Yamada, T., Tajima, H. and Matsumiya, T. (2009) Molecular and functional characterization of choline transporter in rat renal tubule epithelial NRK-52E cells. *Arch. Biochem. Biophys.* **485**, 88-96.
- Yamada, T., Inazu, M., Tajima, H. and Matsumiya, T. (2011) Functional expression of choline transporter-like protein 1 (CTL1) in human neuroblastoma cells and its link to acetylcholine synthesis. *Neurochem. Int.* **58**, 354-365.
- Yara, M., Iwao, B., Hara, N., Yamanaka, T., Uchino, H. and Inazu, M. (2015) Molecular and functional characterization of choline transporter in the human trophoblastic cell line JEG-3 cells. *Placenta* **36**, 631-637.
- Yen, C. L., Mar, M. H. and Zeisel, S. H. (1999) Choline deficiency-induced apoptosis in PC12 cells is associated with diminished membrane phosphatidylcholine and sphingomyelin, accumulation of ceramide and diacylglycerol, and activation of a caspase. *FASEB J.* **13**, 135-142.
- Zhang, Y. (2013) Epidemiology of esophageal cancer. *World J. Gastroenterol.* **19**, 5598-5606.